

Argonne National Laboratory

IRRADIATION AND POSTIRRADIATION ANNEALING OF SOME ALUMINUM-BASE FUELS

by

C. F. Reinke

RECEIVED

Property of

JAN 7 1964

Argonne National Laboratory
Idaho Library

LEGAL NOTICE

This report was prepared as an account of Government sponsored work. Neither the United States, nor the Commission, nor any person acting on behalf of the Commission:

- A. Makes any warranty or representation, expressed or implied, with respect to the accuracy, completeness, or usefulness of the information contained in this report, or that the use of any information, apparatus, method, or process disclosed in this report may not infringe privately owned rights; or*
- B. Assumes any liabilities with respect to the use of, or for damages resulting from the use of any information, apparatus, method, or process disclosed in this report.*

As used in the above, "person acting on behalf of the Commission" includes any employee or contractor of the Commission, or employee of such contractor, to the extent that such employee or contractor of the Commission, or employee of such contractor prepares, disseminates, or provides access to, any information pursuant to his employment or contract with the Commission, or his employment with such contractor.

ARGONNE NATIONAL LABORATORY
9700 South Cass Avenue
Argonne, Illinois 60440

IRRADIATION AND POSTIRRADIATION ANNEALING
OF SOME ALUMINUM-BASE FUELS

by

C. F. Reinke

Final Report - Metallurgy Program 6.1.35

A portion of the material contained in this report has been
reported in the following Metallurgy Division Reports:

<u>Report No.</u>	<u>Pages</u>	<u>Date</u>
ANL-5975	20	1958
ANL-6516	141-142	December 1961
ANL-6677	122-123	December 1962

September 1963

Operated by The University of Chicago
under
Contract W-31-109-eng-38.
with the
U. S. Atomic Energy Commission

TABLE OF CONTENTS

	<u>Page</u>
ABSTRACT	7
INTRODUCTION.	7
FABRICATION HISTORY	8
EXPERIMENTAL PROCEDURE	9
I. Irradiation Experiments	9
II. Annealing Studies	10
EXPERIMENTAL RESULTS AND DISCUSSION.	13
I. Aluminum-39 w/o U_3O_8 Dispersion	13
A. Postirradiation Examination.	13
B. Postirradiation Annealing	21
C. U_3O_8 -Aluminum Reaction	23
D. Discussion	25
II. Aluminum-17.3 w/o Uranium Alloy	25
A. Postirradiation Annealing	25
B. Metallographic Examination.	28
C. Discussion	31
III. General Comparison between the Alloy and Dispersion Systems	35
CONCLUSIONS.	36
ACKNOWLEDGEMENTS	36
REFERENCES.	37
APPENDIX	39

LIST OF FIGURES

<u>No.</u>	<u>Title</u>	<u>Page</u>
1.	Typical Dispersion Specimen Used in the Annealing Studies . .	9
2.	Schematic Drawing of Assembled Irradiation Capsule	10
3.	Effective Specimen Flux for Position MTR A-1-NW	10
4.	Typical Alloy Specimens Used in the Annealing Studies	11
5.	Aluminum-39 w/o U_3O_8 Dispersion Specimens Used in the Annealing Studies	12
6.	As-irradiated Condition of Specimens ED-1 through ED-9 . .	13
7.	As-fabricated Structure of U_3O_8 -Aluminum Dispersion Specimens.	16
8.	Specimen ED-1 after Irradiation to 0.20×10^{20} Fissions/cc Burnup at 55°C.	17
9.	Specimen ED-7 after Irradiation to 0.88×10^{20} Fissions/cc Burnup at 85°C.	18
10.	Specimen ED-1 after Irradiation	19
11.	Specimen ED-1 after Irradiation	19
12.	Specimen ED-1 after Irradiation	20
13.	Specimen ED-7 after Irradiation	20
14.	Specimen ED-7 after Irradiation	20
15.	Specimen ED-6 at Conclusion of Annealing Study	22
16.	Severe Blistering on Specimen W-12-TE	27
17.	Blistering on Specimen W-12-TES.	27
18.	Growth of Fuel Core out of Cladding on Specimen W-12-6 . .	27
19.	Specimen W-12-6 Showing Particles of UAl_4 in Aluminum- rich Matrix.	29

LIST OF FIGURES

<u>No.</u>	<u>Title</u>	<u>Page</u>
20.	Specimen W-12-6 Showing Particles of UAl_4 in Aluminum-rich Matrix.	30
21.	UAl_4 Particles in Aluminum Matrix of Specimen W-12-TES. .	31
22.	Void Formation in Specimen W-12-TES	31
23.	Specimen W-12-TES Showing Void Formation along Line of UAl_4 Particles	32
24.	Aluminum-Uranium Phase Diagram.	33
25.	Swelling in Aluminum-17 to 20 w/o Uranium Alloy Specimens as a Function of Burnup and Temperature.	34

LIST OF TABLES

<u>No.</u>	<u>Title</u>	<u>Page</u>
I.	Chemical and Isotopic Analyses of U_3O_8 -Aluminum Dispersion Specimens	8
II.	Irradiation History of U_3O_8 Dispersion Specimens	10
III.	Comparison of Pre- and Postirradiation Density Measurements on Specimens ED-1 through ED-9.	14
IV.	Comparison of Pre- and Postirradiation Dimensional Measurements on Specimens ED-1 through ED-9.	14
V.	Comparison of Pre- and Postirradiation Weights of Specimens ED-1 through ED-9.	15
VI.	Annealing History of Irradiated 39 w/o U_3O_8 -Aluminum Dispersion Specimens	21
VII.	Annealing History of Unirradiated 39 w/o U_3O_8 -Aluminum Dispersion Specimens	23
VIII.	X-ray Diffraction Analyses of Unirradiated U_3O_8 -Aluminum Control Specimens	24
IX.	Annealing History of Irradiated Aluminum-17.3 w/o Uranium Alloy Specimens	26
X.	Annealing History of Unirradiated Aluminum-17.3 w/o Uranium Alloy Specimens	28

IRRADIATION AND POSTIRRADIATION ANNEALING OF SOME ALUMINUM-BASE FUELS

by

C. F. Reinke

ABSTRACT

Irradiated specimens of 39 w/o U_3O_8 dispersed in aluminum and of aluminum-17.3 w/o uranium alloy were annealed. Each specimen was partially clad with aluminum.

Gross swelling was not observed for the aluminum-39 w/o U_3O_8 dispersion specimens for burnup and annealing temperature levels ranging up to 1.0×10^{20} fissions per cc and 550°C , respectively. Small volume increases were found, however, and these were attributed to the aluminum reduction of U_3O_8 , which is accompanied by measurable volume increases. X-ray diffraction analyses confirmed the reaction between the U_3O_8 and the aluminum matrix. The dispersion specimens and, in particular, the U_3O_8 particles sintered during irradiation at temperatures from 55 to 90°C in an effective thermal-neutron flux of between 1 and 3×10^{13} nv.

Annealing at 550°C produced severe localized blistering on specimens of aluminum-17.3 w/o uranium alloy having burnups of 5.9×10^{20} fissions per cc. Similar conditions produced only a small uniform volume increase when the burnup was 1.4×10^{20} fissions per cc. The observed stability is attributed to a defect structure in the compound UAl_4 in which unoccupied uranium sites trap fission products and, in particular, fission product gases.

INTRODUCTION

One of the most important characteristics of a reactor fuel material is dimensional stability during irradiation. Metallic and cermet fuels if heated during or after irradiation reach a temperature at which large volume increases of the unrestrained solid materials occur in a relatively short time, i.e., they reach the swelling temperature. Therefore, operation at or above this temperature is not feasible without restraint. The useful operating temperature can be extended by suitable cladding or jacketing of the fuel core; but there are practical limitations on the amount of

restraint that can be incorporated into the design of a fuel element. Thus, a knowledge of the swelling temperature of a fuel is essential in defining its operating limitations. To obtain this information for two aluminum-base fuels, a series of annealing studies were made with irradiated aluminum-39 w/o U_3O_8 dispersion specimens and with irradiated aluminum-17.3 w/o uranium alloy.

FABRICATION HISTORY

The U_3O_8 -aluminum dispersion specimens were made as thin strips by hot extruding a powder mixture consisting of 39 w/o of U_3O_8 in aluminum.^(1,2) This type of fuel has been used in the Argonaut Reactor.⁽³⁾ Prior to mixing with the aluminum powder, the U_3O_8 was calcined overnight at 1000°C in air and ground to minus 100 mesh. The aluminum and U_3O_8 powders were then mixed and ball milled overnight to assure proper blending, after which they were loaded into an aluminum can. Prior to extrusion, the billets were heated to 480°C and held at that temperature for 12 to 14 hr. The extruded specimens had a thin aluminum cladding which varied from sample to sample and ranged from practically no cladding to about 0.006 in. maximum. The cut edges of the samples were left unclad. Chemical and isotopic analyses were made of the blended powders and finished specimens. The results are tabulated in Table I.

Table I

CHEMICAL AND ISOTOPIC ANALYSES OF U_3O_8 -ALUMINUM DISPERSION SPECIMENS

Specimen	Powder Core, %					Extruded Specimen, % U
	U	U^{234}	U^{235}	U^{236}	U^{238}	
ED-1 to ED-3	33.7 ± 0.7	0.130 ± 0.002	19.1 ± 0.2	0.126 ± 0.002	80.6 ± 0.2	30.58 ± 0.09
ED-4 to ED-6	33.4 ± 0.7	0.127 ± 0.003	19.0 ± 0.3	0.124 ± 0.003	80.7 ± 0.3	29.44 ± 0.06
ED-7 to ED-9	33.4 ± 0.7	0.127 ± 0.003	19.0 ± 0.3	0.124 ± 0.003	80.7 ± 0.3	29.32 ± 0.06

The 17.3 w/o uranium-aluminum alloy specimens were cut from a plate which had been irradiated in the ANL-2 loop in the MTR.⁽⁴⁾ The plate was manufactured by the same procedures and with the same materials used in the manufacture of the SL-1 core.⁽⁵⁻⁷⁾ The fuel core consisting of 2S aluminum with alloying additions in the following nominal amounts: 17.5 w/o uranium, 2.0 w/o nickel, and 0.5 w/o iron, was vacuum melted and cast into a graphite mold. The casting was conditioned, hot rolled at

580°C, and then cold rolled to final size. The cladding material was M-388 aluminum alloy, which consists of 2S aluminum with an addition of 1% of nickel. The core and cladding components were assembled in a "picture frame" and bonded by the silicon bonding technique.⁽⁸⁾ The bonded assembly was reduced to finish thickness by hot rolling at 550°C, followed by a cold sizing pass.

EXPERIMENTAL PROCEDURE

I. Irradiation Experiments

Figure 1 illustrates the geometry of the U_3O_8 dispersion specimens used in the studies. The dispersion specimens were encapsulated with NaK in capsules similar to the one shown in Figure 2. Each capsule contained one sample. The capsules were irradiated in MTR position A-1-NW from December 7, 1957 to July 7, 1958 for a total of 156.4 days at full power. Figure 3 is a plot of the location of each specimen versus the effective thermal-neutron flux in the position. The plot is based on Cs^{137} burnup analyses of specimens ED-1, ED-2, and ED-7 together with flux-monitor data which were obtained from each capsule. The data do not provide an indication of maximum or minimum flux values during irradiation; thus the flux listed is an average value throughout the period. Table II lists the irradiation history for each specimen based on the average flux values given in Figure 3. The irradiation temperatures were taken from a plot of the calculated central specimen temperature versus the power density, which was based on an electrical-geometrical analogue study of the capsule configuration.

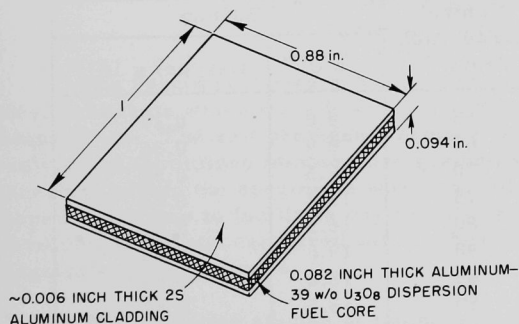
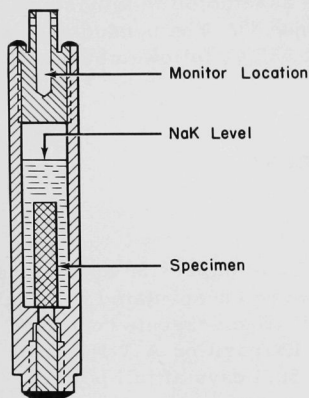


Figure 1

Typical Dispersion Specimen
Used in the Annealing Studies

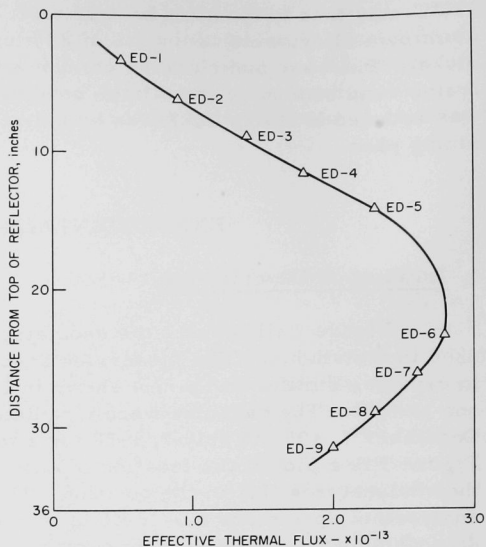
106-7094

The irradiation history of the 17.3 w/o uranium-aluminum alloy specimens is given in detail in Reference 4. In general, the plate from which the specimens were obtained was irradiated in the ANL-2 Argonne High Pressure Water Loop in the MTR for 125 full-power days and achieved a maximum total atom burnup of 1.0 percent as determined by radiochemical burnup analyses.



106-1760

Figure 2. Schematic Drawing of Assembled Irradiation Capsule. The drawing is not to scale.



106-7095

Figure 3. Effective Specimen Flux for Position MTRA-1-NW

Table II

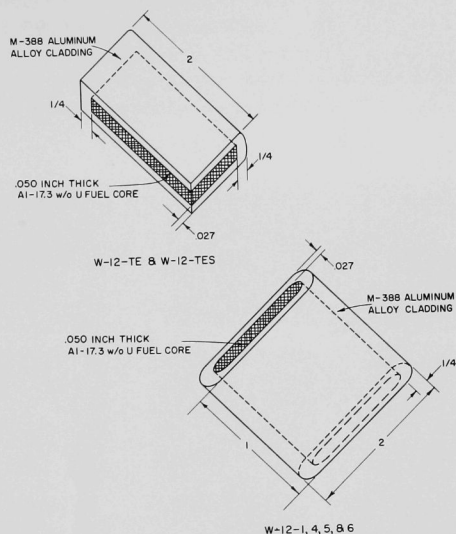
IRRADIATION HISTORY OF U_3O_8 DISPERSION SPECIMENS

Capsule	Specimen No.	Central Irradiation Temp, °C	Burnup	
			a/o U^{235}	(fiss/cc) $\times 10^{-20}$
ANL-6-89	ED-1	55	4.0	0.20
ANL-6-90	ED-2	60	6.9	0.36
ANL-6-91	ED-3	70	10.5	0.54
ANL-6-92	ED-4	75	13.2	0.64
ANL-6-93	ED-5	80	16.5	0.81
ANL-6-94	ED-6	90	19.6	0.95
ANL-6-95	ED-7	85	18.4	0.88
ANL-6-96	ED-8	80	16.5	0.80
ANL-6-97	ED-9	75	14.6	0.71

II. Annealing Studies

Figure 4 illustrates the geometry of the alloy specimens used in the annealing studies. The dispersion specimens used in the annealing studies are shown in Figure 5. The studies were conducted in salt pots

heated by electric-resistance furnaces which were controlled by thermocouples situated between the pot and the furnace. A thermocouple, located inside a well in each pot, recorded the temperature of the salt and thus that of the specimens. The maximum temperature variation observed during each anneal was $\pm 10^{\circ}\text{C}$, and usually the temperature remained within $\pm 5^{\circ}\text{C}$ of the desired value.



106-7093

Figure 4. Typical Alloy Specimens Used in the Annealing Studies

The specimens were placed, along with unirradiated control samples, in baskets which were lowered into the salt after it had stabilized at temperature. The salt provided a protective atmosphere during the annealing and minimized temperature gradients. At the completion of each annealing period the specimens were washed and rinsed in water, and dipped in acetone to facilitate drying. Dimensions and immersion densities were then taken and compared with the pre-test values to determine the magnitude of any changes.

The annealing studies at temperatures up to and including 365°C utilized a salt containing approximately 45 percent sodium nitrite (NaNO_2) and 55 percent potassium nitrate (KNO_3). The annealing studies at 500°C and 550°C utilized a salt containing equal parts of potassium and sodium nitrate.

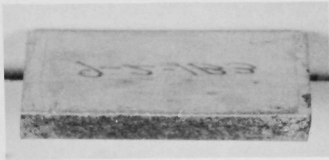
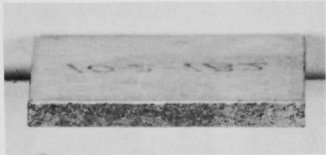


		Specimen	Burnup, (fiss/cc) $\times 10^{-20}$	Irradiation Temperature, °C
 24423	2X	ED-6	0.95	90
 24425	2X	ED-8	0.80	80
 24426	2X	ED-9	0.71	75
 24420	2X	ED-3	0.54	70

Figure 5. Aluminum-39 w/o U_3O_8 Dispersion Specimens Used in the Annealing Studies. Photos show unclad edge and numbered face of square specimens.

EXPERIMENTAL RESULTS AND DISCUSSION

I. Aluminum-39 w/o U_3O_8 DispersionA. Postirradiation Examination

The postirradiation examination revealed that the U_3O_8 dispersion specimens were in excellent condition. Figure 6 shows the specimens after irradiation. Their condition is not surprising as the irradiation temperatures and burnups were comparatively low. There is little doubt that the specimens would have operated satisfactorily at higher temperatures and burnup levels.



24417

1X

Figure 6. As-irradiated Condition of Specimens ED-1 through ED-9.

The observed changes in density and dimensions are presented in Tables III, IV, and V. With but one exception, ED-7, the samples densified under the conditions of irradiation. The reason for the anomalous value for ED-7 is not known; however, it is not believed to be a valid change. There was no correlation between these changes and either burnup or specimen irradiation temperature.

The length and width of each specimen remained constant while the thickness decreased. In all cases, although the changes were small and close to the precision of the measurements, the general trend for a decrease

in thickness was well established. The dimensional data are difficult to interpret except in a general way because, due to their geometry, the specimens had a considerable range in values even before irradiation.

Table III

COMPARISON OF PRE- AND POSTIRRADIATION DENSITY MEASUREMENTS ON SPECIMENS ED-1 THROUGH ED-9

Specimen	Density, ^(a) g/cc		
	Pre	Post	% $\Delta \rho$
ED-1	3.414	3.425	+0.32
ED-2	3.486	3.494	+0.23
ED-3	3.448	3.464	+0.46
ED-4	3.348	3.359	+0.33
ED-5	3.387	3.400	+0.38
ED-6	3.372	3.391	+0.56
ED-7	3.312	3.290	-0.66
ED-8	3.374	3.380	+0.18
ED-9	3.376	3.379	+0.09

(a) The estimated precision of the measurements is ± 0.004 g/cc

Table IV

COMPARISON OF PRE- AND POSTIRRADIATION DIMENSIONAL MEASUREMENTS ON SPECIMENS ED-1 THROUGH ED-9

Specimen	Dimensions, in. ^(a)		
	Length	Width	Thickness
ED-1	Pre 1.002-1.003	0.880	0.099-0.100
	Post 0.998-1.005	0.880-0.882	0.098-0.101
ED-2	Pre 0.987-0.988	0.883	0.101
	Post 0.988-0.989	0.882-0.883	0.099-0.100
ED-3	Pre 0.978-0.983	0.884-0.885	0.100
	Post 0.981-0.982	0.884-0.885	0.098
ED-4	Pre 1.009-1.010	0.884-0.885	0.100-0.102
	Post 1.008	0.884	0.099
ED-5	Pre 1.014-1.023	0.886	0.102-0.103
	Post 1.016-1.021	0.886-0.889	0.100
ED-6	Pre 1.022-1.034	0.885-0.887	0.100-0.101
	Post 1.029-1.034	0.888-0.889	0.098
ED-7	Pre 1.004-1.015	0.881	0.099-0.100
	Post 1.008-1.015	0.882	0.097-0.098
ED-8	Pre 0.996-1.002	0.884	0.101-0.102
	Post 1.001-1.003	0.882-0.885	0.100
ED-9	Pre 0.984-0.990	0.882-0.883	0.099-0.100
	Post 0.988-0.990	0.884	0.098-0.099

(a) The values represent a minimum of two readings for each dimension. Each individual value has a precision of ± 0.001 in.

Table V

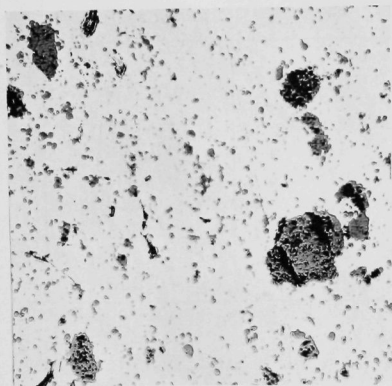
COMPARISON OF PRE- AND POSTIRRADIATION WEIGHTS
OF SPECIMENS ED-1 THROUGH ED-9

Specimen	Weight, g		
	Pre	Post	Change
ED-1	4.651	4.651	-
ED-2	4.725	4.726	+0.001
ED-3	4.628	4.635	+0.007
ED-4	4.670	4.674	+0.004
ED-5	4.820	4.825	+0.005
ED-6	4.805	4.822	+0.017
ED-7	4.574	4.579	+0.005
ED-8	4.676	4.678	+0.002
ED-9	4.568	4.571	+0.003

The microstructure shown in Figure 7 is typical of the U_3O_8 dispersion specimens before irradiation. As can be seen, the larger particles of U_3O_8 were quite porous. There was no obvious evidence of any reaction between the U_3O_8 and the aluminum matrix. However, as seen in the photomicrograph at 750X, a careful examination at the higher magnification did reveal reaction zones surrounding some of the smaller particles. X-ray diffraction analyses confirmed the existence of these zones and indicated that approximately 10% of the oxide present was UO_2 . The UO_2 probably formed prior to extrusion during the soaking period of 12 to 14 hr at 480°C by aluminum reduction of the U_3O_8 .

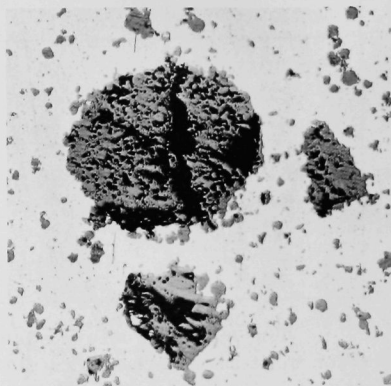
The increase in density, decrease in thickness, increase in weight, and postirradiation appearance of the U_3O_8 particles are all compatible with the hypothesis that sintering occurred during irradiation. Initially it was thought that NaK corrosion may have produced the observed densification; however, an attempt to explain the density, thickness, and weight data on the basis of NaK corrosion was not successful. Since the face of each specimen was clad with aluminum, a preferential removal of aluminum by NaK corrosion would have the effect of increasing the density of the composite specimen and decreasing the specimen thickness concurrently. The increase in weight would then be attributed to oxidized NaK coolant picked up by the exposed fuel at the edges of the specimen. The calculations were based on measured weights and densities, and indicated that if the observed decrease in thickness were attributed to aluminum corrosion, the increase in density of the composite, due to the loss of the lower-density aluminum cladding, still would not be equal to the observed densification. Furthermore, the surface appearance of the specimens,

shown in Figure 6, and the low overall specimen irradiation temperature of approximately 100°C indicate that corrosion of the aluminum cladding was not a problem. Calculations indicate that the temperature drop within individual oxide particles is less than 10°C. Thus, all the data indicate that sintering had indeed occurred even though the irradiation temperatures were approximately 100°C.



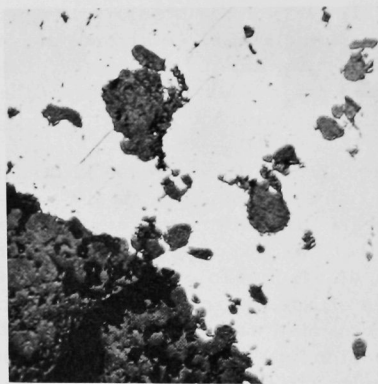
EI-573

100X



EI-574

250X

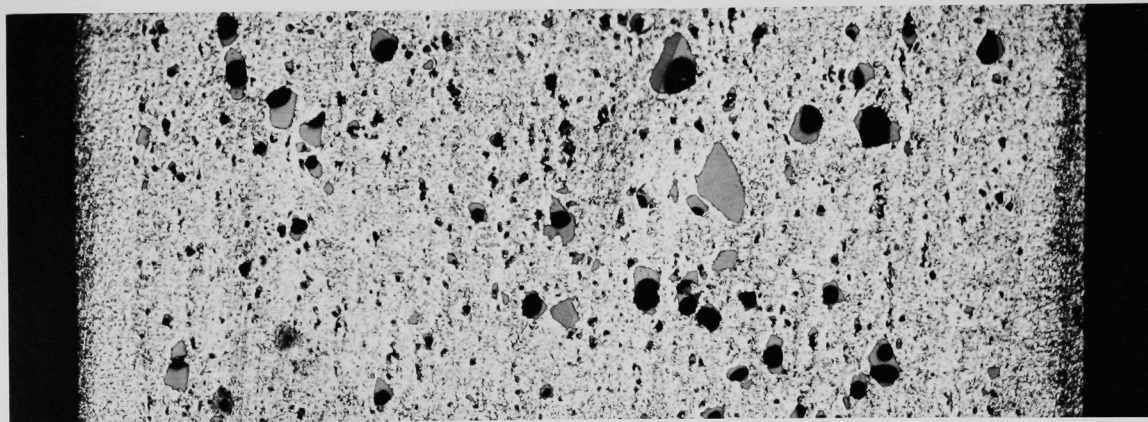


EI-576

750X

Figure 7. As-fabricated Structure of U_3O_8 -Aluminum Dispersion Specimens. The photos show the specimens in the as-polished condition.

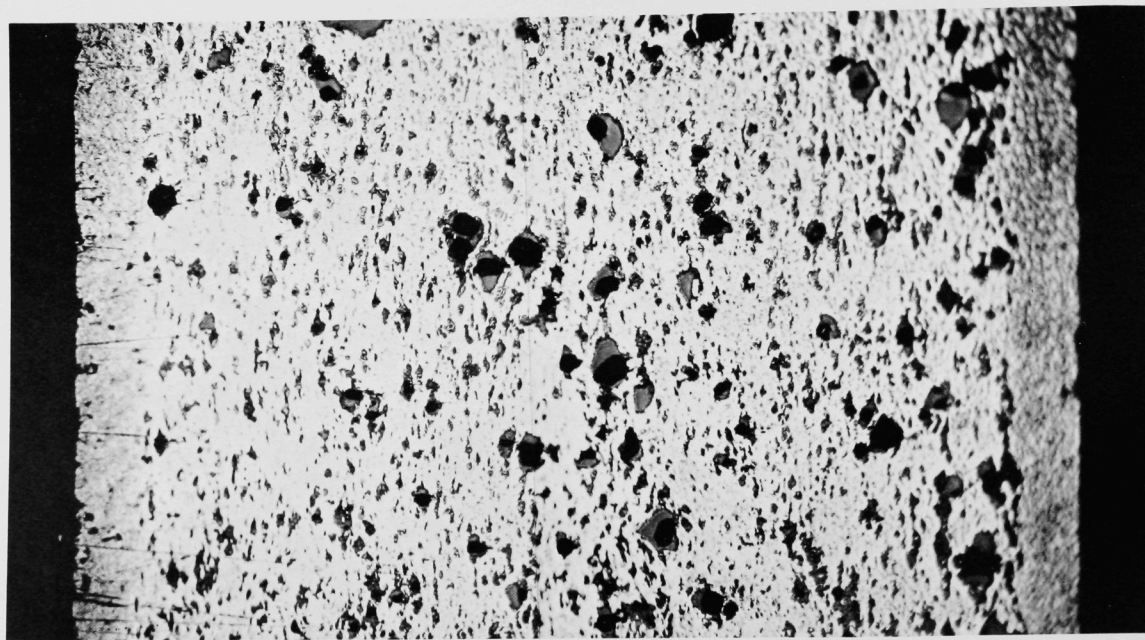
Figures 8 through 14 are typical of the structure existing after irradiation. As can be seen, the U_3O_8 particles had undergone sintering even though the irradiation temperatures were estimated well below the



EI-862

75X

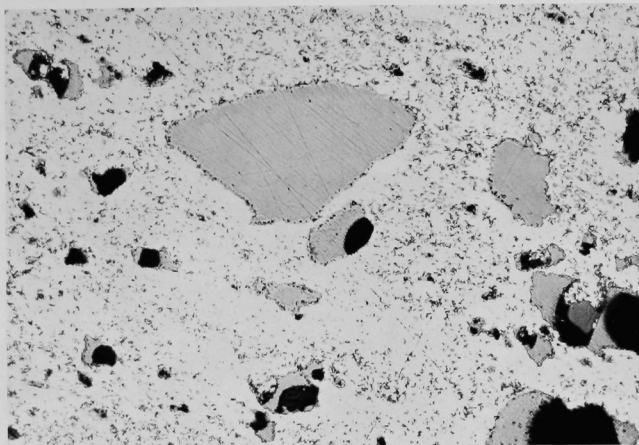
Figure 8. Specimen ED-1 after Irradiation to 0.20×10^{20} Fissions/cc Burnup at 55°C .



EI-863

75X

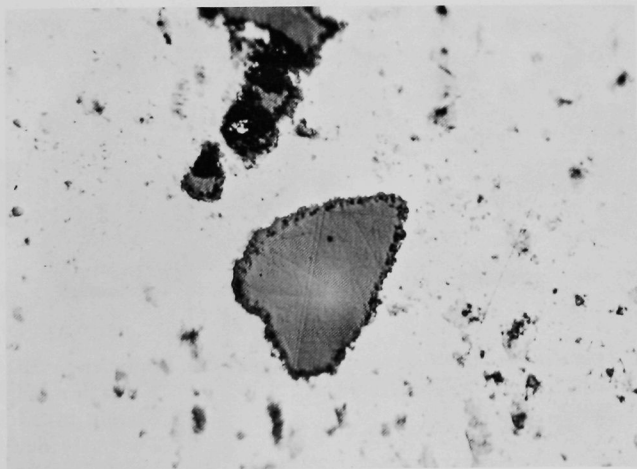
Figure 9. Specimen ED-7 after Irradiation to 0.88×10^{20} Fissions/cc Burnup at 85°C .



EI-864

250X

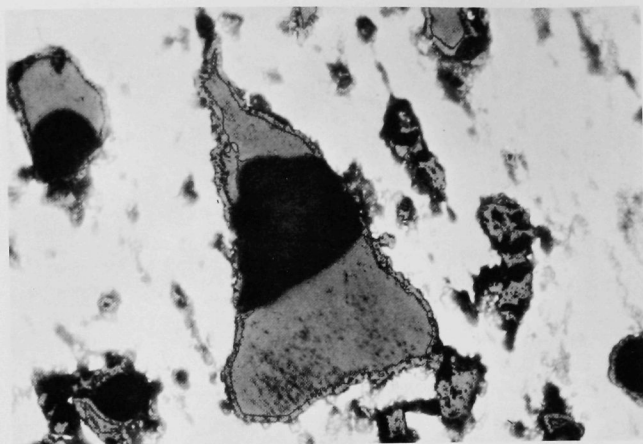
Figure 10. Specimen ED-1 after Irradiation. Note sintering in U_3O_8 particles. Sample in as-polished condition.



EI-795

250X

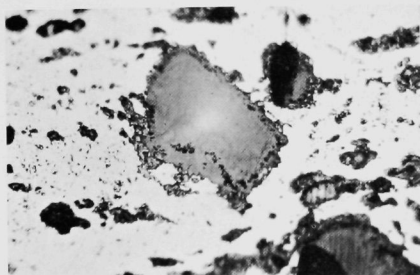
Figure 11. Specimen ED-1 after Irradiation. Note sintering in U_3O_8 particle. Sample in as-polished condition.



EI-865

500X

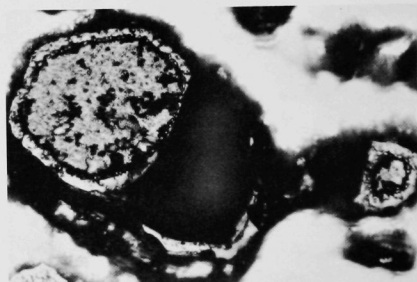
Figure 12. Specimen ED-1 after Irradiation. Specimen etched in 2% HF solution, showing zone surrounding particle.



EI-866

250X

Figure 13. Specimen ED-7 after Irradiation. As-polished condition.



EI-796

500X

Figure 14. Specimen ED-7 after Irradiation. Specimen etched in 2% HF solution. Porosity due to burnup.

minimum temperature of approximately 800°C necessary to initiate sintering of the oxide. This low-temperature sintering phenomena, called radiation sintering, has been observed before.(9-11) The mechanism by which it occurs, however, is not thoroughly understood.(12) The fact that shrinkage occurred suggests that either lattice diffusion or plastic flow is an important mechanism

involved in the sintering process. The lattice diffusion model, discussed by Burke,⁽¹³⁾ seems the most reasonable of the two. The low irradiation temperature may have enhanced diffusion rates by producing an increased concentration of vacancy-interstitial pairs or by changing the location of sinks for vacancies to migrate.

Examination of the figures also reveals that the porosity within the irradiated particles was concentrated at the outer edges. As can be seen in Figure 12, the porosity may concentrate in apparent reaction zones surrounding the particles.

B. Postirradiation Annealing

The results of the annealing studies are tabulated in Table VI. Annealing temperatures up to 365°C produced initial volume increases of between 0.5 to 1 percent ΔV . However, after 360 hr the measured densities were close to the pre-test values and indicate no measurable change in volume at that time. Volume increases of 1 and 4 percent were observed with samples annealed for approximately 500 hr at 500°C and 550°C, respectively. Figure 15 shows that specimen ED-6, annealed at 550°C, had

Table VI
ANNEALING HISTORY OF IRRADIATED 39 w/o U_3O_8 -ALUMINUM DISPERSION SPECIMENS

Specimen	Burnup		Annealing Temp, °C(a)	Time at Temp, hr	Cumulative Time at Temp, hr	Weight, ^(b) g	Density, ^(b) g/cc	Total % ΔV (f)	Dimensions, ^(b) in.		
	(fissions/cc) $\times 10^{-20}$	% U^{235}							Length	Width	Thickness
ED-6	0.95	19.6	550	0	0	4.815(d)	3.383(d)	-	1.028	0.887	0.094
				24	24	4.819	3.382	NMC	1.034	0.887	0.095
				69	93	4.919(c)	3.308(c)	+1.1	1.051	0.899	0.096
				115	208	5.756(c)	3.990(c)	+4.9	1.186	0.929-1.122	0.118
				115	323	5.937(e)	2.960(e)	+4.8	1.210	0.945-1.104	0.118
				94	417	5.992	2.962	+4.2	1.202	0.966-1.087	0.115
				94	511	6.018	2.956	+4.2	1.199	0.962-1.101	0.117
ED-8	0.80	16.5	500	0	0	4.674(c)	3.379(c)	-	0.998	0.885	0.094
				24	24	4.674(c)	3.395(c)	-0.5	1.006	0.884	0.095
				69	93	4.678	3.392	-0.4	0.999	0.885	0.094
				116	209	4.679	3.393	-0.4	1.002	0.885	0.094
				115	324	4.693(c)	3.373(c)	NMC	1.006	0.888	0.095
				209	533	4.739(c)	3.316(c)	+1.1	1.011	0.898	0.093
ED-9	0.71	14.6	365	0	0	4.602	3.363	-	0.997	0.887	0.095
				24	24	4.571	3.403	-	0.987	0.887	0.094
				72	96	4.566	3.396	+0.2	0.992	0.890	0.093
				144	240	4.566	3.391	+0.4	0.988	0.886	0.095
				120	360	4.561	3.403	NMC	0.989	0.885	0.092
ED-3	0.54	10.5	210	0	0	4.656	3.456	-	1.006	0.889	0.094
				24	24	4.627	3.473	-	0.980	0.888	0.094
				72	96	4.630	3.441	+0.9	0.980	0.885	0.094
				146	242	4.628	3.474	NMC	0.982	0.884	0.094
				120	362	4.624	3.476	NMC	0.981	0.882	0.093

(a) The temperature did not vary more than $\pm 10^\circ\text{C}$ at any time during the test.

(b) The precision of the measurements is: weight, ± 0.002 g; density, ± 0.004 g/cc; dimensions, ± 0.001 in.

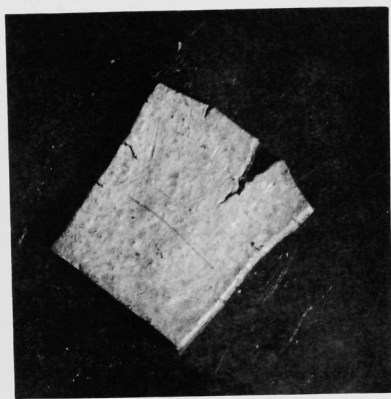
(c) Represents the average of two measurements.

(d) Represents the average of six measurements.

(e) Represents the average of three measurements.

(f) Calculated from the expression $\% \Delta V = \left[\frac{\rho_i}{\rho_f} - 1 \right] \times 100$, where ρ_i and ρ_f are the initial and final densities, respectively.

cracked badly. The cracking was first noticed at the close of the third annealing period, at which time the specimen had accumulated 208 hr at temperature. The cracks did not seem to enlarge appreciably with further annealing. The other specimens were in good condition at the close of the tests. The precision of the weight and density measurements was determined by a series of fifteen measurements made on a similar irradiated but unannealed specimen. The data indicate a standard deviation of ± 0.002 g for weight and of ± 0.004 g/cc for density measurements.



EI-185

1X

Figure 15. Specimen ED-6 at Conclusion of Annealing Study.

were not completely successful. However, examination of the specimens showed that the oxide had been removed during the initial annealing period. This was also indicated by the decrease in weight and increase in density of the specimens. The weights and densities after the initial annealing period compare favorably with the measurements taken immediately after irradiation. Therefore, in calculating the percent change in volume, the initial density of specimens ED-3 and ED-9 was taken as more truly represented by the densities after the first annealing period, and these were used in calculating the subsequent volume changes.

Specimens ED-6 and ED-8 with their respective control samples C-4 and C-3 increased in weight as the tests progressed. It was apparent that the salt was adhering to the samples. Therefore, where necessary, the measured weights and volumes given in Tables VI and VII were corrected, as shown in the appendix, to account for the salt. The corrected weights and volumes were then used to calculate the density of the specimen, and this density was used to determine any change which occurred due to the additional annealing time. The density of the salt was taken as 2.18 g/cc.

The data for the unirradiated control samples, annealed concurrently with the test specimens, are given in Table VII. It can be seen from the data that the unirradiated specimens decreased in density. The higher the annealing temperature, the greater the decrease in density or increase in volume. These volume increases are associated, in a way not fully understood, with the reaction between the U_3O_8 particles and the

aluminum matrix. The quantity of hydrogen present in the specimens was unknown. However, if it was significant it could also have contributed to the observed volume increases.

Table VII
ANNEALING HISTORY OF UNIRRADIATED 39 w/o U_3O_8 -ALUMINUM DISPERSION SPECIMENS

Specimen	Annealing Temp. ^(a) °C	Time at Temp, hr	Cumulative Time at Temp, hr	Weight ^(b) g	Density ^(b) g/cc	Total % ΔV ^(d)	Thickness ^(b) in.
C-4	550	0	0	10.740	3.374	-	0.091
		24	24	10.777	3.262	+3.3	
		69	93	10.800	3.260	+3.2	
		115	208	10.818	3.263	+3.0	
		115	323	10.853 ^(c)	3.250 ^(c)	+3.3	
		94	417	10.853	3.258	+3.0	
C-3	500	94	511	10.874	3.259	+2.9	0.101-0.103
		0	0	9.182	3.376	-	0.091
		24	24	9.202 ^(c)	3.319 ^(c)	+1.6	
		69	93	9.226	3.320	+1.4	
		116	209	9.243	3.329	+1.1	
		115	324	9.251 ^(c)	3.324 ^(c)	+1.1	
C-2	365	209	533	9.268	3.329	+0.9	0.97-0.99
		0	0	10.105	3.382	-	0.096
		24	24	10.107	3.370	+0.4	
		72	96	10.107	3.358	+0.7	
		144	240	10.110	3.352	+0.9	
		120	360	10.109	3.360	+0.6	0.096-0.100
C-1	210	0	0	9.258	3.382	-	0.095
		24	24	9.257	3.376	+0.2	
		72	96	9.263	3.366	+0.5	
		146	242	9.259	3.363	+0.6	
		120	362	9.257	3.369	+0.4	0.095-0.099

(a) The temperature did not vary more than $\pm 10^\circ\text{C}$ at any time during the test.

(b) The precision of the measurements is: weight ± 0.002 g; density, ± 0.004 g/cc; thickness, ± 0.001 in.

(c) Represents the average of two measurements.

(d) Calculated from the expression $\% \Delta V = \left[\left(\frac{\rho_i}{\rho_f} \right) - 1 \right] 100$ where ρ_i and ρ_f are the initial and final densities respectively.

C. U_3O_8 -Aluminum Reaction

It has been observed that U_3O_8 and UO_2 react with aluminum at temperatures between 500 and 600°C .⁽¹⁴⁻¹⁶⁾ UO_2 and Al_2O_3 form by the aluminum reduction of the U_3O_8 . The UO_2 is also reduced by the aluminum with the formation of U-Al intermetallics and more Al_2O_3 . The reaction proceeds in steps with the eventual conversion of all the uranium present to the intermetallic compound UAl_4 . Calculations based upon the balanced equations and theoretical densities of the reactants and products indicate that overall volume decreases should accompany the reaction. These decreases have not been observed, however. In fact, the reaction produces sizable volume increases. This apparent anomaly may be explained if one assumes that the reaction products are somewhat less than theoretically dense. This may be possible if the reaction proceeds by the Kirkendall mechanism.

Sections from both the irradiated and unirradiated U_3O_8 -aluminum specimens used in the annealing studies were dissolved in hot concentrated sodium hydroxide solution. Each oxide residue was washed and filtered; and a sample taken for X-ray diffraction analysis. X-ray diffraction analyses of the U_3O_8 obtained from the irradiated specimens were not successful because of film fogging due to their activity. The results of the analyses on the unirradiated specimens are given in Table VIII. The presence of UO_2 was detected in all cases. The data indicate that the concentration of UO_2 was dependent upon temperature and time. In some instances the metallographic examination also revealed a dependence upon particle size and shape. However, for the most part, the metallographic examinations at magnifications up to 750X did not reveal any reaction zones surrounding the U_3O_8 particles. These results are in general agreement with other experiments(14-16) in which it was also demonstrated that the oxide manufacturing process and additives such as TiO_2 or CaF_2 affect the reaction. The relative quantities of each phase present were estimated based on the observed line intensities.

Table VIII

X-RAY DIFFRACTION ANALYSES OF UNIRRADIATED
 U_3O_8 -ALUMINUM CONTROL SPECIMENS

Specimen No.	Annealing History	Phases Present
U	None	90% U_3O_8 + 10% UO_2
C-1	362 hr at 210°C	85% U_3O_8 + 15% UO_2
C-2	360 hr at 365°C	80% U_3O_8 + 20% UO_2
C-3	533 hr at 500°C	60% U_3O_8 + 40% UO_2 + trace UAl_3
C-4	511 hr at 550°C	40% U_3O_8 + 50% UO_2 + 10% UAl_3 + trace of UAl_4

The dependence of the UO_2 concentration upon temperature can be seen by comparing the results of annealing studies conducted for approximately equivalent times but at different temperatures. The quantity of UO_2 increased as the annealing temperature increased. The as-fabricated sample had 10% UO_2 present which probably formed during the soaking period of 12 to 14 hr at 480°C prior to extrusion, whereas the UO_2 concentration had increased to 40% after 533 hr at 500°C. Thus, the quantity of UO_2 increases as the length of time at a given temperature increases. The data also indicate that reduction of the UO_2 begins after about 40% of the U_3O_8 has been reduced.

D. Discussion

In its initial stages the reaction between aluminum and U_3O_8 produces UO_2 and, as the reduction of UO_2 progresses, U-Al intermetallics begin to form. This reaction leads to measurable volume increases.

Although X-ray diffraction analyses could not be run with the irradiated specimens to verify the presence of UO_2 , it is speculated that the volume increases noted for the irradiated specimens can, at least in part, be attributed to this reaction also. In particular, specimens ED-3, ED-8, and ED-9 along with their unirradiated controls exhibited similar volume increases as a result of the annealing. Therefore, it is speculated that the observed increases were due chiefly to the U_3O_8 -aluminum reaction, plus the agglomeration of any residual hydrogen, and not to the agglomeration of fission product gases.

Specimen ED-6 exhibited a volume increase slightly in excess of that associated with the U_3O_8 -aluminum reactions. This excess was probably the result of fission gas agglomeration. ED-6 also cracked badly during the course of the annealing study, for reasons not known. However, it is not believed to be associated with either the U_3O_8 -aluminum reactions or fission gas agglomeration. It might be related to prior fabrication history in some way.

The U_3O_8 -aluminum dispersion system seems resistant to gross swelling caused by fission gas agglomeration for burnups up to at least 1.0×10^{20} fissions per cc and temperatures up to 550°C . Small volume increases will occur with fuel operated between 210°C and 550°C due to the aluminum reduction of the U_3O_8 and intermetallic formation. After approximately 500 hr, this amounts to about 1% at 500°C and to 3% at 550°C .

II. Aluminum-17.3 w/o Uranium Alloy

A. Postirradiation Annealing

Figure 4 illustrates the geometry of the specimens used in the annealing studies. The experimental procedures were identical with those described in the preceding section for the U_3O_8 -aluminum dispersions; in fact, the alloy and dispersion specimens were annealed together. For each annealing temperature, the specimens were chosen with approximately equivalent burnups so that information would be obtained, not only about the swelling temperature of each material, but also sufficient for comparing the two systems.

The results of the annealing studies on the irradiated specimens are tabulated in Table IX. Volume increases occurred in all specimens annealed at 550°C. As can be seen in Figures 16 to 18, at a burnup of 5.9×10^{20} fissions per cc swelling occurred as severe localized blistering whereas at a burnup of 1.4×10^{20} fissions per cc the volume increase was uniform in nature. Specimens with burnups ranging from 0.41×10^{20} to 1.2×10^{20} fissions per cc showed a tendency towards a slight uniform increase in volume for annealing temperatures in the range from 210°C to 500°C. The precision of the weight and density measurements was determined by a series of fifteen measurements made on similar irradiated but unannealed material. The data indicate a standard deviation of ± 0.002 g for the weight and of ± 0.003 g/cc for the density measurements.

Table IX
ANNEALING HISTORY OF IRRADIATED ALUMINUM-17.3 w/o URANIUM ALLOY SPECIMENS

Specimen	Burnup		Annealing Temp, (a) °C	Time at Temp, hr	Cumulative Time at Temp, hr	Weight, (b) g	Density, (b) g/cc	Total % ΔV (e)	Dimensions, (b) in.		
	(Fissions/cc) $\times 10^{-20}$	% U ²³⁵							Length	Width	Thickness
W-12-TE	5.9	45.1	550	0	0	10.405	2.856	-	2.055	1.001	0.111
				94	94	10.430	2.426	+17.7	2.082	0.989	0.112-0.219
				1.5	95.5	10.422	2.419	+18.0	2.079	0.986	0.119-0.220
				2	97.5	10.434	2.416	+18.2	2.076	0.981-1.003	0.107-0.209
				3.5	101	10.478	2.413	+18.3	2.076	0.986-1.006	0.128-0.215
				3	104	10.525	2.386	+19.5	2.087	0.980-1.003	0.131-0.228
				46	150	10.631	2.360	+20.8	2.074	0.977-1.009	0.128-0.230
				36	186	10.753	2.352	+21.1	2.088	0.980-1.008	0.126-0.228
				114	300	10.928	2.321	+22.6	2.094	0.983-1.021	0.139-0.244
				71	371	11.065	2.308	+23.3	2.101	0.984-1.021	0.133-0.249
W-12-TES	5.9	45.1	550	0	0	4.986	2.809	-	2.051	0.497	0.104
				1.5	1.5	4.952	2.791	+ 0.6	2.054	0.493	0.104
				2	3.5	4.945	2.767	+ 1.5	2.042	0.491-0.505	0.096-0.106
				3.5	7	4.944	2.760	+ 1.8	2.045	0.487-0.505	0.098-0.105
				3	10	4.944	2.744	+ 2.4	2.051	0.490-0.504	0.098-0.105
				94	104	4.997	2.667	+ 5.3	2.072	0.504-0.510	0.101-0.133
				46	150	5.020	2.636	+ 6.6	2.011	0.502-0.511	0.098-0.124
				36	186	5.033	2.627	+ 6.9	2.070	0.502-0.513	0.095-0.117
				114	300	5.058	2.616	+ 7.4	2.078	0.497-0.552	0.104-0.114
				71	371	5.071	2.616	+ 7.4	2.076	0.505-0.514	0.097-0.133
W-12-6	1.4	10.8	550	0	0	10.415(c)	2.890(c)	-	1.024	2.001	0.105
				24	24	10.382	2.887	NMC	1.024	1.999	0.106
				69	93	10.367	2.881	+ 0.3	1.024	2.004	0.105
				115	208	10.353	2.881	+ 0.3	1.027	2.008	0.103
				115	323	10.364(d)	2.865(d)	+ 0.9	1.031	2.000	0.103
				94	417	10.354	2.860	+ 1.0	1.032	2.003	0.102
				94	511	10.356	2.850	+ 1.4	1.034	2.004	0.102
				0	0	10.141(d)	2.889(d)	-	1.005	2.000	0.105
				24	24	10.120(d)	2.896(d)	-	1.004	1.998	0.103
				69	93	10.111	2.895	NMC	1.006	1.998	0.103
W-12-5	1.2	8.8	500	116	209	10.102	2.896	NMC	1.005	1.996	0.103
				115	324	10.103(d)	2.891(d)	+ 0.2	1.002	1.996	0.103
				209	533	10.093	2.892	+ 0.1	1.005	1.999	0.103
				0	0	9.897	2.904	-	0.987	1.996	0.105
				24	24	9.887	2.903	NMC	0.990	1.995	0.104
W-12-4	0.77	5.8	365	72	96	9.887	2.891	+ 0.4	0.989	1.995	0.104
				144	240	9.885	2.888	+ 0.6	0.989	1.997	0.104
				120	360	9.883	2.896	+ 0.3	0.991	1.995	0.104
				0	0	10.293	2.904	-	1.022	1.993	0.104
W-12-1	0.41	3.2	210	24	24	10.281	2.903	NMC	1.022	1.991	0.105
				72	96	10.380	2.905	NMC	1.022	1.992	0.104
				146	242	10.283	2.898	+ 0.2	1.022	1.993	0.105
				120	362	10.277	2.897	+ 0.2	1.020	1.994	0.103

(a) The temperature did not vary more than $\pm 10^\circ\text{C}$ at any time during the test.

(b) The precision of measurements is: weight, ± 0.002 g; density, ± 0.003 g/cc; dimensions, ± 0.001 in.

(c) Is the average of six measurements.

(d) Is the average of two measurements.

(e) Based on the assumption of no weight change and calculated from the expression $\% \Delta V = \left[\frac{\rho_i}{\rho_f} - 1 \right] \times 100$, where ρ_i and ρ_f are the initial and final densities, respectively. NMC means no measurable change.



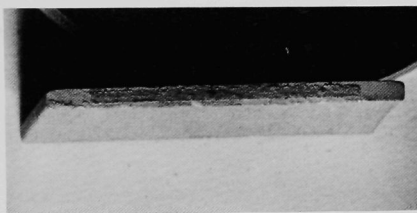
EI-229 ~1X
Burnup 5.9×10^{20} fissions/cc
Annealing Conditions 371 hr at 550°C

Figure 16. Severe Blistering on Specimen W-12-TE.



EI-223 ~1X
Burnup 5.9×10^{20} fissions/cc
Annealing Conditions 371 hr at 550°C

Figure 17. Blistering on Specimen W-12-TES.



EI-196 ~1X
Burnup 1.4×10^{20} fissions/cc
Annealing Conditions 511 hr at 550°C

Figure 18. Growth of Fuel Core out of Cladding on Specimen W-12-6.

Data on the unirradiated control specimens, given in Table X, indicate a slight volume increase for annealing temperatures up to 365°C . The cause of this increase in volume is not known. The significance of the increase, however, is questionable, as the data also indicate that similar material annealed at significantly higher temperatures had not swelled. The specimens were in excellent condition at the close of the tests. There was no evidence of any corrosive attack by the annealing salts.

The irradiated specimens had varying quantities of oxide present on their surfaces at the start of the tests. Most of the oxide was removed after the initial annealing period. However, specimens W-12-TE and W-12-TES retained some of their surface oxides and, in addition, picked up annealing salt, which accounts for the sizable weight increases which were noted. The measured weights and volumes, given in Table IX, were corrected to account for the salt and these corrected weights and volumes were used to calculate the density of the specimen. This corrected density was then used to determine any change which occurred due to annealing. The density of the salt was taken as 2.18 g/cc .

Table X

ANNEALING HISTORY OF UNIRRADIATED ALUMINUM-17.3 w/o URANIUM ALLOY SPECIMENS

Specimen	Annealing Temp, ^(a) °C	Time at Temp, hr	Cumulative Time at Temp, hr	Weight, ^(b) g	Density, ^(b) g/cc	Total % ΔV ^(c)	Thickness, ^(b) in.
C-44	550	0	0	13.568 ^(d)	2.834 ^(d)	-	0.77
		24	24	13.565	2.838	-0.1	0.76
		69	93	13.560	2.836	NMC	0.76
		115	208	13.560	2.840	-0.2	0.75
		115	323	13.570 ^(d)	2.834 ^(d)	NMC	0.74
		94	417	13.563	2.836	NMC	0.74
C-33	500	94	511	13.564	2.835	NMC	0.73
		0	0	14.757	2.931	-	0.77
		24	24	14.756 ^(d)	2.932 ^(d)	NMC	0.77
		69	93	14.759	2.929	NMC	0.76
		116	209	14.755	2.934	NMC	0.76
		115	324	14.757 ^(d)	2.930 ^(d)	NMC	0.75
C-22	365	209	533	14.759	2.934	NMC	0.76
		0	0	14.809	2.936	-	0.82
		24	24	14.808	2.932	+0.1	
		72	96	14.810	2.932	+0.1	
		144	240	14.812	2.932	+0.1	
C-11	210	120	360	14.809	2.925	+0.4	0.82
		0	0	13.058	2.927	-	0.81
		24	24	13.057	2.924	NMC	
		72	96	13.058	2.928	NMC	
		146	242	13.058	2.927	NMC	
		120	362	13.057	2.917	+0.3	0.81

(a) The temperature did not vary more than $\pm 10^\circ\text{C}$ at any time during the test.

(b) The precision of the measurements is: weight, ± 0.002 g; density, ± 0.003 g/cc; thickness, ± 0.001 in.

(c) Based on the assumption of no weight change and calculated from the expression: $\% \Delta V = \left[\frac{\rho_i}{\rho_f} - 1 \right] 100$, where ρ_i and ρ_f are the initial and final densities, respectively. NMC means no measurable change.

(d) \bar{x} is the average of two measurements.

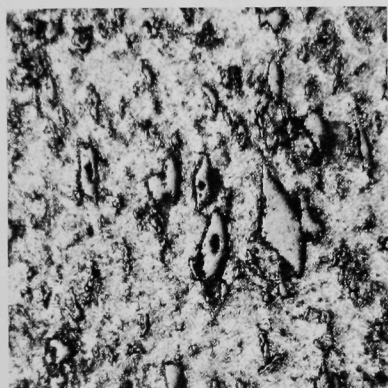
There was a difference in the ratio of fuel to aluminum in the two specimens with burnup amounting to 5.9×10^{20} fissions per cc. This accounts for the observed difference in the total $\% \Delta V$ between the specimens and points up the fact that since all the specimens were clad, the $\% \Delta V$ is dependent upon the geometry and the quantity of aluminum present. Thus, although similar volume increases could have occurred in the fuel core, a specimen containing a larger fraction of aluminum would appear to have a lower total $\% \Delta V$. The data are thus useful in establishing the swelling temperature but not the absolute magnitude of the change to be expected unless specimens of similar geometry are compared.

B. Metallographic Examination

Irradiated specimens W-12-6 and W-12-TES were examined metallographically at the conclusion of the annealing period. The specimens were mounted with cold-setting plastic and ground to a 600 grit finish on silicon carbide paper dressed with paraffin. They were then rough polished on Nylon cloth impregnated with $6\text{-}\mu$ diamond abrasive and final polished with Microcloth on a plastic lap with Magomet polishing compound.

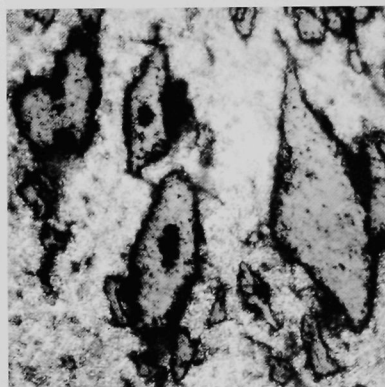
The specimens were examined in both the as-polished and etched condition. A swab etch was employed with either a 10 percent NaOH or a 2 percent HF solution. The sodium hydroxide solution removed deformed metal without etching the UAl_4 particles appreciably, whereas the HF solution had a tendency to attack the UAl_4 particles also.

Figures 19 and 20 are typical of the UAl_4 particles in specimen W-12-6. After etching the particles stood out in relief. The particles had retained their characteristic diamond shape, and there was no evidence of any cracks within the particles or the aluminum-rich matrix. Some porosity was present in the particles, but this is to be expected at a burnup level



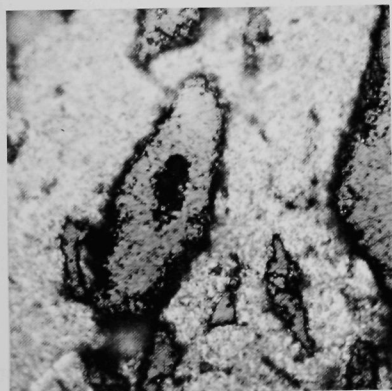
EI-787

250X



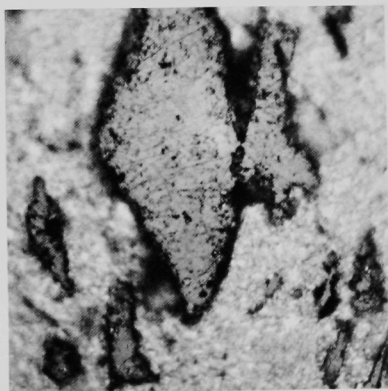
EI-792

500X



EI-790

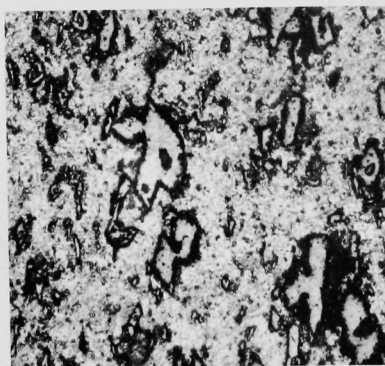
750X



EI-791

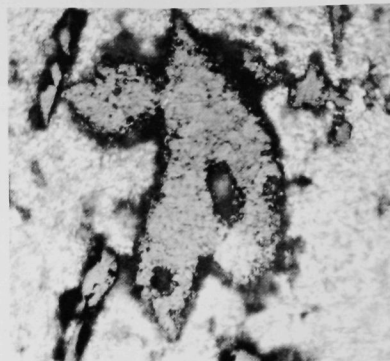
750X

Figure 19. Specimen W-12-6 Showing Particles of UAl_4 in Aluminum-rich Matrix. Specimen was annealed for 511 hr at 550°C. Etched with NaOH. All structures photographed under selective tint.



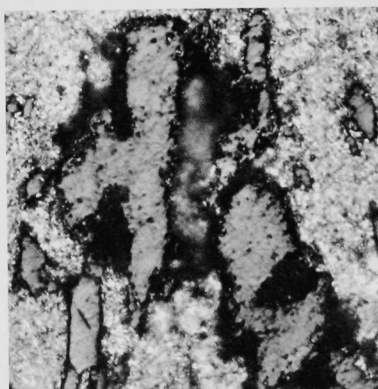
EI-786

250X



EI-789

750X



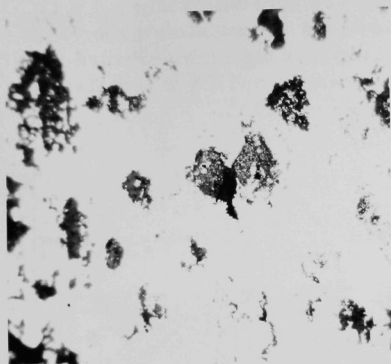
EI-788

750X

Figure 20. Specimen W-12-6 Showing Particles of UAl_4 in Aluminum-rich Matrix. Specimen was annealed for 511 hr at 550°C . Etched with NaOH. All structures photographed under selective tint.

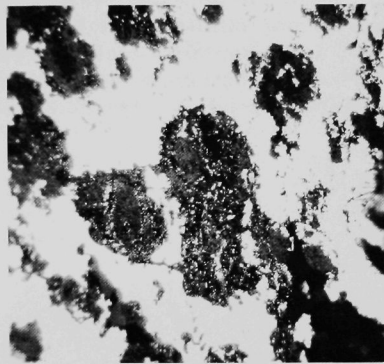
of 10 percent of the U^{235} . In general the microstructure revealed that the matrix and the uranium bearing phase were in good condition after irradiation to a burnup of 1.4×10^{20} fissions per cc and subsequent annealing at 550°C for 511 hr.

The microstructure of specimen W-12-TES, which had a burnup about four times that of W-12-6, can be seen in Figure 21. The UAl_4 particles are considerably more porous than those of W-12-6, and many of the particles have lost their original shape. Figures 22 and 23 are macro- and microphotographs showing the void areas in the sample.



EI-885

250X



EI-886

500X

Figure 21. UAl_4 Particles in Aluminum Matrix of Specimen W-12-TES.
Note porosity present.



EI-793

3X

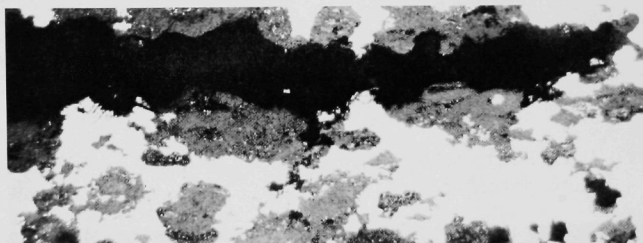
Figure 22. Void Formation in Specimen W-12-TES.

Figure 22 also shows blistering in the aluminum cladding itself. The blistering probably did not originate within the cladding. It most probably originated in the fuel core and then extended into the cladding at a point of weakness. It can be seen in the microphotograph that void formation occurred along lines of UAl_4 particles.

C. Discussion

Based on the results of the annealing studies, the aluminum-17.3 w/o uranium system exhibited a remarkable resistance to swelling, even considering the fact that the fuel core was clad with 0.027 in. of aluminum. At a burnup of 5.9×10^{20} fissions per cc, a temperature fairly close to the melting point of the aluminum was reached before the onset of gross swelling was evident. Similar conditions produced only a small

uniform volume increase when the burnup was approximately 1.4×10^{20} fissions per cc. Similar blistering was observed on an aluminum-17.5 w/o uranium alloy fuel plate irradiated in a high temperature water loop.⁽¹⁷⁾ The burnup in the blistered area was about 6.6×10^{20} fissions/cc, with a corresponding estimated temperature of 540°C.



EI-883

250X

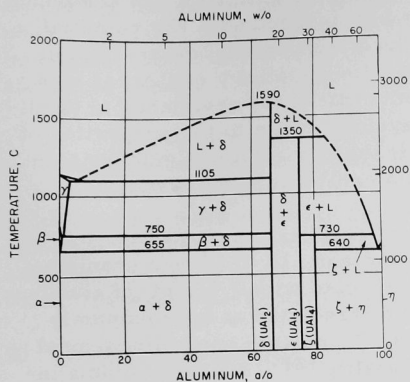


EI-794

500X

Figure 23. Specimen W-12-TES Showing Void Formation along Line of UAl_4 Particles.

An examination of the uranium-aluminum phase diagram, shown in Figure 24, indicates that the aluminum-17.3 w/o uranium alloy is really



EI-892

Figure 24. Aluminum-Uranium Phase Diagram.

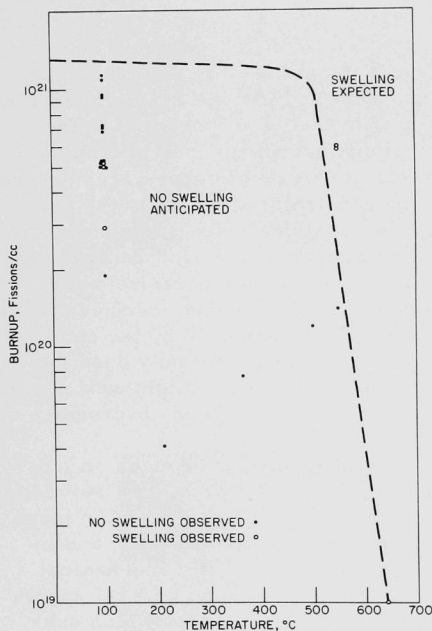
the quantity of gas needed to produce swelling. The volume occupied by the gas would increase until the pressure exerted was balanced by the constraint afforded by the aluminum matrix and cladding. Not only does the physical geometry of the specimens indicate that swelling might well occur as blistering in localized areas, but such blistering has been observed.

A lack of swelling at elevated temperature is taken as an indication of the absence of sizable amounts of gases in the free state surrounding the UAl₄ particles. Resistance to swelling would thus seem to be more dependent upon the properties of the intermetallic compound UAl₄, and in particular to its ability to retain fission gases, than upon the mechanical properties of the aluminum matrix and cladding or upon the general specimen geometry. Some data have been observed at low burnups which substantiate the ability of UAl₄ particles to retain fission gases even at elevated temperatures.⁽¹⁸⁾ In this work there was negligible fission gas release from particles of UAl₄ annealed at temperatures below 600°C. Gas release was usually rapid, however, on initial heating to temperatures above about 650°C.

X-ray diffraction analyses indicate that the intermetallic compound UAl₄ has a body-centered orthorhombic structure with a unit cell of $a = 4.41 \text{ \AA}$, $b = 6.27 \text{ \AA}$, and $c = 13.71 \text{ \AA}$.^(19,20) Each uranium atom has as its nearest neighbors thirteen aluminum atoms at a minimum interatomic distance of about 3 \AA . It has also been observed that the measured

a dispersion of the intermetallic compound UAl₄ in an essentially uranium-free aluminum matrix. It is anticipated that any fission gases released from a UAl₄ particle would be present at the aluminum-UAl₄ particle interface. Once the gas bubbles exceed a critical size, these gases can be expected to follow the perfect gas law. Thus, the pressure exerted by the gases would be directly proportional to the quantity of gas present and the absolute temperature, and inversely proportional to the volume occupied. It is speculated that at elevated temperatures, where the constraint afforded by the aluminum is small, the presence of these gases would produce swelling; the higher the temperature, the less

and theoretical densities do not agree.⁽¹⁹⁾ The theoretical density is 6.12 g/cc, and the measured densities were 5.7 ± 0.3 g/cc. This discrepancy is in part explained by assuming a defect structure for the compound UAl_4 in which some of the uranium sites are unoccupied. The potential ability of these sites to trap fission products and, in particular, fission product gases may in part explain the excellent stability of UAl_4 at high burnup and temperatures. It is noteworthy that if the resistance to swelling of the aluminum-17.3 w/o uranium system is due to the properties of the UAl_4 intermetallic compound, then all the compositions with uranium concentrations of up to 20 a/o should also exhibit this resistance.



106-7280

Figure 25. Swelling in Aluminum-17 to 20 w/o Uranium Alloy Specimens as a Function of Burnup and Temperature.

approximately 0.030 in. of X-8001 aluminum alloy.

Recent data on platelets of aluminum-18 to 23 w/o uranium fuel, clad with 0.015 in. of aluminum and irradiated at approximately 100°C, indicate good dimensional stability.⁽²¹⁾ Average volume increases of about 2 to 4 percent were noted for burnups ranging up to 11.3×10^{20} fissions per cc. It is concluded from these results and those discussed above that swelling in the aluminum-17.3 w/o uranium system should be more dependent upon temperature than upon burnup. Figure 25 is a plot of burnup versus temperature for the aluminum-uranium system of about 17 to 20 w/o uranium. The data at 100°C were obtained from Ref. 21, which described tests of samples having 0.020-in.-thick fuel cores clad with 0.015 in. of various aluminum alloy claddings. The upper temperature limit was assumed. It was based on the observed data of Reynolds⁽¹⁸⁾ which indicated sizable quantities of fission gas release even at low burnup when particles of UAl_4 were annealed at about 640°C. The intervening data are the results of the present annealing studies on 0.050-in.-thick fuel cores clad with ap-

The plot is separated into two regions. In the region below the line combinations of burnup and temperature are postulated which are stable, whereas those above the line are combinations of burnup and

temperature which will produce swelling. Swelling, for purposes of the plot, is defined as severe localized blistering or general volume increases exceeding 10 percent per atom percent burnup. The line is dotted to emphasize the fact that the data points are not extensive; thus, the curve must be considered tentative until verified by additional data at elevated temperature and burnup.

The form of swelling taken by the aluminum-17.3 w/o uranium specimens used in the annealing studies was severe localized blistering. It is believed that the blistering originated in a stringered area when fission product gases were released from the UAl_4 particles and readily joined with other gases from adjacent particles because the aluminum did not provide sufficient mechanical strength at the temperatures involved to restrain them. Two such areas can be seen in Figure 23.

III. General Comparison between the Alloy and Dispersion Systems

The alloy and dispersion systems cannot be compared directly on the basis of the data developed during the present annealing study because of the varying amounts of restraint afforded by the differing geometries. Although at temperatures above 500°C , at which the strength afforded by the aluminum is not great, direct comparisons may yield reasonable approximations of the relative capabilities of the two systems.

For burnups up to about 1×10^{20} fissions per cc and temperatures ranging up to 500°C , the 39 w/o U_3O_8 -aluminum dispersion system had slightly larger volume increases than the aluminum-17.3 w/o uranium alloy system. This difference may be due to the fact that the alloy specimens were more highly restrained. Actually, if it were not for the reaction between the aluminum and the U_3O_8 , the dispersion specimens would have exhibited better resistance than the alloy. Thus, although the dispersion system may be slightly more resistant to fission gas swelling in this range, the volume increase accompanying the aluminum- U_3O_8 reaction makes it slightly less resistant to overall swelling than the alloy.

The large difference in burnup between specimens annealed at 550°C does not allow a comparison to be drawn between the two systems.

It has been noted that at temperatures above 210°C the aluminum matrix and U_3O_8 react with the eventual formation of UAl_4 . Measurable volume increases accompany this reaction, and data indicate that at completion a volume increase of about 4% can be expected.⁽¹⁵⁾ Aluminum systems with up to 20 a/o uranium exist as the intermetallic compound UAl_4 in an essentially uranium-free aluminum matrix. Since the uranium in the U_3O_8 will eventually revert to UAl_4 , the alloy system would seem to be basically more resistant to volume increases, for it does away with the volume increase accompanying the aluminum- U_3O_8 reaction.

CONCLUSIONS

1. Specimens containing 39 w/o U_3O_8 dispersed in aluminum were in excellent condition after being irradiated to burnups ranging up to 1×10^{20} fissions per cc at temperatures between 55 and 90°C.
2. Based on the annealing studies, 39 w/o U_3O_8 -aluminum dispersions are resistant to swelling for burnup and temperature levels up to at least 1×10^{20} fissions per cc and 550°C, respectively.
3. U_3O_8 reacts with aluminum at temperatures as low as 210°C with the formation of UO_2 , Al_2O_3 , and U-Al intermetallic compounds. Temperature, time, and particle size are variables which affect the rate of the reaction.
4. Volume increases accompany the U_3O_8 -aluminum reaction. After approximately 500 hr the volume increases amounted to 1% at 500°C and to 3% at 550°C. After approximately 360 hr the volume increases amounted to about 0.5% at 210°C and 365°C.
5. The dispersion specimens and, in particular, the U_3O_8 particles sintered during irradiation at temperatures from 55 to 90°C in an effective thermal neutron flux of between 1 and 3×10^{13} nv.
6. Based on the annealing studies, 17.3 w/o uranium-aluminum specimens having burnups up to at least 1.4×10^{20} fissions per cc are resistant to swelling at temperatures as high as 550°C.
7. Based on the annealing studies, 17.3 w/o uranium-aluminum specimens with burnups equal to 5.9×10^{20} fissions per cc will swell rapidly at 550°C. The swelling occurs as severe localized blistering.

ACKNOWLEDGEMENTS

The author wishes to acknowledge the efforts of the designated individuals who contributed to the following phases of the study:

D. E. Walker	Specimen Fabrication
J. H. Kittel	Capsule Irradiations
F. J. Tebo	Electrical Geometrical Analogue Study
J. A. Horak	Flux Monitor Analyses
W. C. Kettman	Data Collection
R. P. Larsen	Burnup Analyses
R. Carlander	Metallography
H. W. Knott	X-ray Diffraction Analyses

REFERENCES

1. J. H. Handwerk, R. A. Noland, and D. E. Walker, Method of Fabrication of Fuel Elements Using Metal Powder and U_3O_8 , U. S. Patent No. 2,805,473 (Sept 1957).
2. R. A. Noland, D. E. Walker, and L. C. Hymes, ASTM Special Technical Publication No. 276, Fabrication of U_3O_8 -Aluminum Dispersion Fuel Elements by Extrusion, p. 336, American Society for Testing Materials (1960).
3. D. H. Lennox and C. N. Kelber, Summary Report on Hazards of Argonaut Reactor, ANL-5647 (1956).
4. J. H. Kittel, C. C. Crothers, and R. Carlander, Irradiation of an Aluminum-Uranium Alloy Fuel Plate under Local Boiling Conditions, ANL-6607 (to be published).
5. R. A. Noland, D. E. Walker, M. Martin, and S. Matras, Manufacture of Fuel Plates and Fuel Assemblies for the Argonne Low Power Reactor, ANL-5965 (to be published).
6. R. A. Noland, Manufacture of Fuel Plates and Fuel Assemblies for the Argonne Low Power Reactor, TID-7559, I 233-244 (1958), Paper presented at Fuel Element Conference at Gatlinburg, Tennessee, May 14-16, 1958.
7. R. L. Salley and W. R. Burt, Jr., Casting and Fabrication of Core Materials for Argonne Low Power Reactor Fuel Elements, ANL-5950 (1959).
8. D. E. Walker, R. A. Noland, F. D. McCuaig, and C. C. Stone, BORAX-IV Reactor: Manufacture of Fuel and Blanket Elements, ANL-5721 (1958).
9. E. W. Hoyt and D. L. Zimmerman, Radiation Effects in Borides, Part II - Fission Sintering of Boride Powders, GEAP-3743 (1962).
10. R. A. Ewing and D. N. Sunderman, Effects of Radiation upon Hafnium Diboride, BMI-1521 (1961).
11. W. K. Barney and B. D. Wemple, Metallography of UO_2 Containing Fuel Elements, KAPL-1836 (1958).
12. E. A. Aitken, Sintering Characteristics in a Radiation Environment, Paper presented at the ASTM Symposium on Radiation Effects in Refractory Fuel Compounds, Atlantic City, New Jersey, June 1961.
13. J. E. Burke, Role of Grain Boundaries in Sintering, J. Am. Cer. Soc., 40(3), 80-85 (1957).
14. A. E. Eiss, Reactivity of Certain Uranium Oxides with Aluminum, SCNC-257 (1958).

15. R. C. Waugh and R. J. Beaver, Recent Developments in the Powder Metallurgy Application of Uranium Oxides to Aluminum Research Reactor Fuel Elements, CF-57-9-60 (1957).
16. R. C. Waugh, The Reaction and Growth of Uranium Dioxide-Aluminum Fuel Plates and Compacts, ORNL-2701 (1959).
17. A. P. Gavin and C. C. Crothers, Irradiation of an Aluminum Alloy-clad, Aluminum-Uranium Alloy-fueled Plate, ANL-6180 (1960).
18. M. B. Reynolds, Fission Gas Behavior in the Uranium-Aluminum System, Nuclear Sci. and Eng., 3, 428-434 (1958).
19. B. S. Borie, Jr., Crystal Structure of UAl_4 , J. of Metals, 3, 800 (1951).
20. A. H. Snell and E. O. Wollan, Quarterly Progress Report for Period Ending March 15, 1950, ORNL-693 (1950).
21. G. W. Gibson and O. I. Shupe, Annual Progress Report on Fuel Element Development for FY 1961, IDO-16727 (1962).

APPENDIX

Method of Correcting Specimen Weights and
Volumes for Salt Pickup

From Table VI the measured weight and density of specimen ED-6 were 6.018 g and 2.956 g/cc, respectively, after annealing for 511 hr at 550°C. The original weight and density were 4.815 g and 3.383 g/cc.

The original specimen weight minus the final specimen weight gives the weight of the salt picked up:

$$6.018 - 4.815 = 1.203 \text{ g} \quad .$$

The volume occupied by the salt is given by

$$\begin{array}{c} \text{volume} \\ \text{of} \\ \text{salt} \end{array} = \frac{\text{weight of salt}}{\text{density of salt}} = \frac{1.203 \text{ g}}{2.18 \text{ g/cc}} = 0.552 \text{ cc} \quad .$$

From the data in Table VI the volume occupied by the specimen plus the salt is

$$\text{volume of specimen + salt} = \frac{6.018}{2.956} = 2.036 \text{ cc} \quad .$$

The corrected volume of the specimen is thus

$$2.036 - 0.552 = 1.484 \text{ cc} \quad .$$

The corrected density is given by

$$\frac{4.815}{1.484} = 3.244 \text{ g/cc} \quad .$$

Thus, the % ΔV is given by $\left[\frac{\rho_i}{\rho_f} - 1 \right] 100 \quad ,$

which for this case is

$$\left[\frac{3.383}{3.244} - 1 \right] 100 = 4.2\% \quad ,$$

as given in Table VI.

ARGONNE NATIONAL LAB WEST



3 4444 00008143 0

x